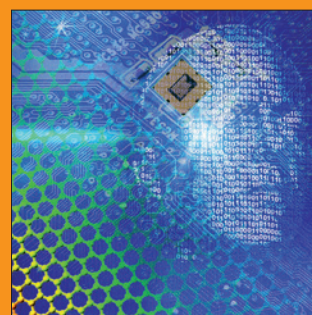
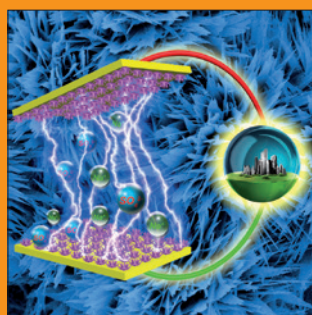
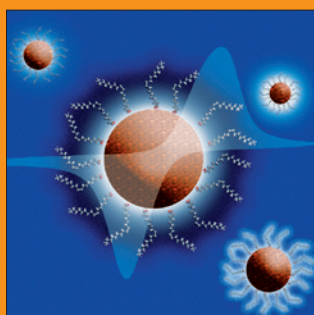
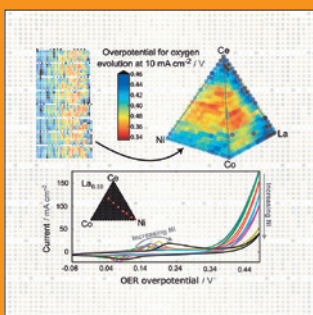
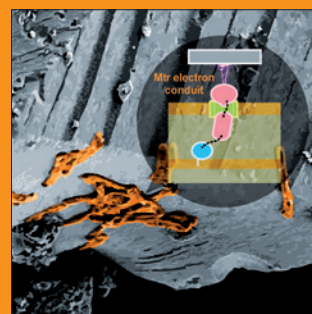
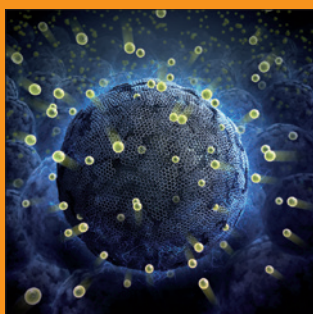
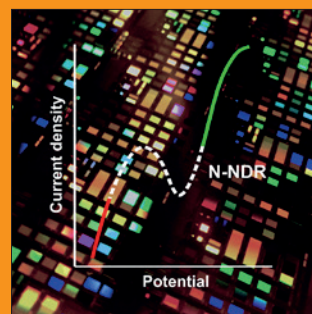
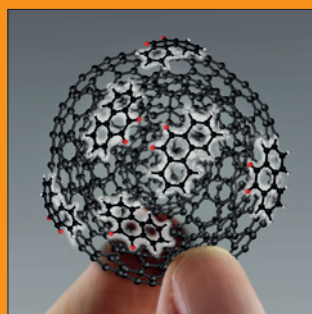
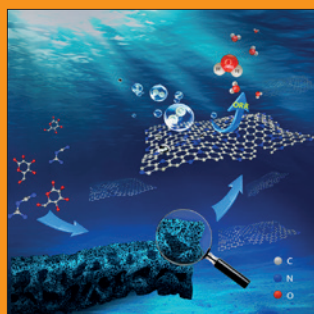
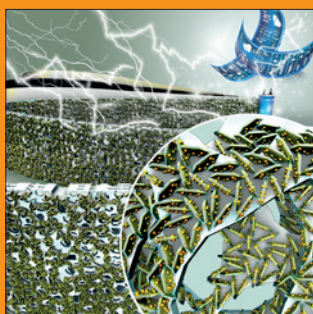


FUNDAMENTALS & APPLICATIONS

# CHEMELECTROCHEM

ANALYSIS & CATALYSIS, BIO & NANO, ENERGY & MORE



## Reprint

A Journal of



WILEY-VCH

[www.chemelectrochem.org](http://www.chemelectrochem.org)

# Electrochemical Oxidation of Theophylline in Organic Solvents: HPLC-PDA-ESI-MS/MS Analysis of the Oxidation Products

Isabella Chiarotto, Leonardo Mattiello, Fabiana Pandolfi, Daniele Rocco, Marta Feroci,\* and Rita Petrucci\*<sup>[a]</sup>

The electrochemical oxidation of theophylline was investigated by controlled potential electrolysis in two different organic solvents and in water for comparison. The anodic oxidation was monitored by cyclic voltammetry in situ and UV-Vis spectrophotometry ex situ and the final electrolyzed solutions were analyzed by tandem mass spectrometry after chromatographic separation with an HPLC-PDA-ESI-MS/MS system. The main oxidation products evidenced as the main diode array chroma-

tographic peaks were tentatively assigned to dimeric forms of theophylline, two of which have never been reported before, on the base of retention time, UV-Vis spectrum, *m/z* ratio in both positive and negative ESI modes and fragmentation pattern. Two chemical paths following the primary mono-electronic anodic oxidation of theophylline to the final evidenced oxidation products have been proposed.

## 1. Introduction

Methylxanthines are widely distributed in nature, being present in a significant number of botanical species. Among these, caffeine (1,3,7-trimethylxanthine), theobromine (3,7-dimethylxanthine) and theophylline (1,3-dimethylxanthine) are mainly available in almost one hundred species, including coffee, cocoa and tea, so that they have been included in human diet since ancient times. Nowadays, these compounds are the most widely consumed alkaloids in human dietary, daily taken in high consumption products as traditional beverages and food, soft and energy drinks and more recently as food supplement. Many systemic effects induced in humans by these natural xanthine derivatives are well known, even if the mechanisms of action have not always been clarified. On the other hand, beneficial effects on human health have been ascribed to these compounds, depending also on their bioavailability and biotransformation in the organism, and the same are currently used as therapeutic tools.<sup>[1]</sup>

Tea species are the main natural source of theophylline (TPH) that is also present in trace amounts in cocoa and coffee beans. Among the physiological mechanisms proposed for methylxanthines, TPH is thought acting mainly as antagonist of adenosine receptors and phosphodiesterase inhibitor.<sup>[2]</sup> Central nervous system (CNS) stimulator as the most popular caffeine,<sup>[3]</sup>

metabolite of caffeine and other naturally occurring alkaloids, TPH has been used in medicine for decades as a drug for the therapy of different respiratory diseases.<sup>[4]</sup> Nowadays, new contexts are being proposed with positive outcomes for caffeine and TPH (Figure 1), and increasing pharmaceutical and

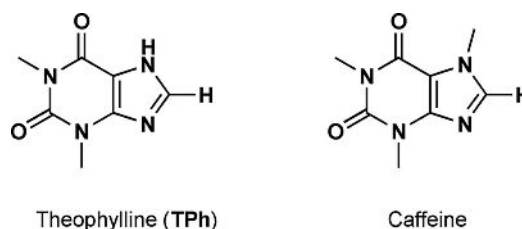


Figure 1. Theophylline and caffeine structures.

therapeutic potentialities are emerging from an always growing number of scientific reports on them. Also the antioxidant capacity of caffeine and TPH, mainly as HO<sup>•</sup> scavenger, has been discussed more recently.<sup>[5–7]</sup>

On the other hand, the wide pharmaceutical employ of TPH in human and in veterinary medicine,<sup>[8]</sup> added to the important industrial processes concerning coffee, cocoa and tea, led to its ubiquitous detection in the aquatic environment, as recently reported.<sup>[9]</sup> Furthermore, several studies reported an acute toxicity to mammals and human, especially when mixed with other pharmaceuticals,<sup>[10–11]</sup> so that TPH can be considered among the emerging pharmaceutical pollutants of aquatic environment.

In the context of oxidation technologies for pollutant degradation, the HO<sup>•</sup> induced oxidation of TPH in water has been recently reported.<sup>[10]</sup> The efficiency of hydroxyl radical mediated destruction of TPH was evaluated in low concentration solution and various degradation products including

[a] Prof. I. Chiarotto, Prof. L. Mattiello, Dr. F. Pandolfi, D. Rocco, Prof. M. Feroci, Prof. R. Petrucci  
Department Scienze di Base e Applicate per l'Ingegneria (SBAI)  
Sapienza University of Rome  
via Castro Laurenziano, 7, 00161, Roma, Italy  
E-mail: marta.feroci@uniroma1.it  
rita.petrucci@uniroma1.it

Supporting information for this article is available on the WWW under <https://doi.org/10.1002/celec.201901071>

An invited contribution to a Special Collection dedicated to *Giornale dell'Elettrochimica Italiana 2019 (GEI2019)*

isomeric xanthenes and uric acids were characterized by LC-QTOF/MS.<sup>[10]</sup> Also the oxidation by Ferrate (VI) has been recently reported and low molecular weight oxidation products were identified by UPLC-QTOF/MS analyses.<sup>[12]</sup>

If few studies on the chemically induced oxidation of TPh have been reported in literature, also the electrochemical oxidation has been sparingly studied,<sup>[7,13]</sup> and more recent electrochemical studies mainly aimed at analytical application.<sup>[14–15]</sup>

As for caffeine, by far the most thoroughly studied methylxanthine (also in organic solvents,<sup>[7,16–19]</sup>) the few reported studies on TPh were mainly carried out in water at different pH.<sup>[20]</sup> Major differences compared to the electrochemical behavior of caffeine were firstly evidenced, as the formation of little amounts of a dimeric form of TPh insoluble in water:<sup>[13]</sup> a one-electron one-proton anodic oxidation of TPh was there supposed, and two oxidative routes were proposed for the electro-generated radical: dimerization or further oxidation to uric acids and degradation derivatives.

A recent study has been reported on the electrochemical oxidation of caffeine and TPh in aprotic medium, considered more suitable to study mechanisms involving radical intermediates.<sup>[7]</sup> Also in this case, some differences were evidenced in the behavior of TPh compared to caffeine, mainly ascribed to the different nature of the radical species resulting from the oxidation of TPh and caffeine. A pattern for possible competitive reactions of the radical species generating from the anodic oxidation of TPh was there proposed.

Due to the involvement of theophylline, as is or as caffeine metabolite, in different field, from physiological effects on human health to therapeutic applications, from potential antioxidant capacity to environmental contamination and to its nature of building block for pharmaceutical application, further investigations on its behavior under oxidative condition are still requested. In particular, the reactivity of the radical species involved in the oxidation of TPh are worthy of attention.

Because of the electrophilic nature of the radical cation, high reactivity with water is expected, as evidenced by the highly oxidized products reported in literature for oxidation of caffeine and TPh,<sup>[13,20]</sup> while dimeric forms were not reported in literature excepted one.<sup>[13]</sup>

In the present work, a systematic study of the oxidation products of TPh aimed to evidence similarities and differences in aprotic and protic medium. The electrochemical oxidation of TPh was carried out by controlled potential electrolysis in acetonitrile and *N,N*-dimethylformamide, also in the presence of stoichiometric amounts of water, the organic solvents providing a more friendly environment for radical species. Electrolysis in water was also performed for a useful comparison. The anodic oxidation was monitored by cyclic voltammetry and UV-Vis spectrophotometry *ex-situ*. All the final electrolyzed solutions were analyzed by tandem mass spectrometry after chromatographic separation with an HPLC-PDA-ESI-MS/MS system (high-performance liquid chromatography-photo diode array-electrospray ionization-tandem mass spectrometry).

## 2. Results

The electrochemical oxidation of TPh was studied by controlled potential electrolysis (CPE) in acetonitrile (ACN) and *N,N*-dimethylformamide (DMF). The two organic solvents were chosen among others in order to solubilize TPh, whose solubility is really low in the majority of organic solvents tested. The anodic behavior of TPh was also studied in aqueous medium, even if already reported in literature,<sup>[13,20]</sup> to get homogeneous data to evidence any differences between the oxidation process in aprotic and protic medium.

Cyclic voltammeteries (CVs), performed to measure the anodic potential value to be used for electrolysis, were carried out on TPh 0.02 M in solvent/supporting electrolyte at a glassy carbon (GC) electrode, at the scan rate of 200 mVs<sup>-1</sup>. A broadened irreversible anodic peak was evidenced in all solvent/supporting electrolyte systems used, as shown in Figures 2a–e (red curves), in agreement with the electrochemical study on TPh in aprotic medium, topic of the previous work recently published.<sup>[7]</sup> The anodic peak potential values were in the range of 1.3–2.0 V, vs saturated calomel electrode (SCE), the lowest value measured in water/KCl (pH = 7) while the highest one was approximately the same in both ACN and DMF, all values in good agreement with literature.<sup>[7,15,21]</sup> Controlled little amounts of water added to the organic solvent/supporting electrolyte solutions did not seem to have a strong influence on the primary anodic oxidation of TPh, the cyclic voltammeteries (Figures 2c and 2e, green curves) resembling those ones recorded in the absence of added water (red curves).

CPEs were carried out using two platinum electrodes in a divided cell, on solutions containing TPh 0.02 M, at the experimental potential value of +2.0 V, vs SCE. All electrolyses were stopped after 1F, consistent with the expected mono-electronic process, and after 2F, to obtain comparable data in protic and aprotic medium, and small amounts of each solution taken for analysis.

Cyclic voltammograms reported in Figures 2a–e (red curves) show that it was not possible to selectively oxidize TPh in our experimental conditions, both in organic and aqueous solvent, as also confirmed by the presence of not negligible residual amounts of TPh after 2F electrolysis (see chromatographic data below). Moreover, after 2F electrolysis the anodic peak current at the potential of TPh was approximately the same of the starting one or higher, as shown by cyclic voltammograms reported in Figures 2a–e (blue curves), suggesting the presence of anodic oxidation products that might be further oxidized at the same applied potential value.

All electrolysis experiments were monitored by UV-Vis spectrophotometry *ex-situ*. UV-Vis spectra of all TPh solvent/supporting electrolyte solutions were recorded on the starting material (red lines), after 1F (black lines) and after 2F (blue lines) electrolysis, as shown in Figures 3a–e, and a different behavior was observed when using an organic solvent or water. In fact, a significant decrease of the TPh characteristic absorbance at  $\lambda_{\max}/274$  nm was observed in both ACN and DMF, with or without added water (Figures 3b–e), while a persistent absorption was evidenced when water/KCl was used (Figure 3a),



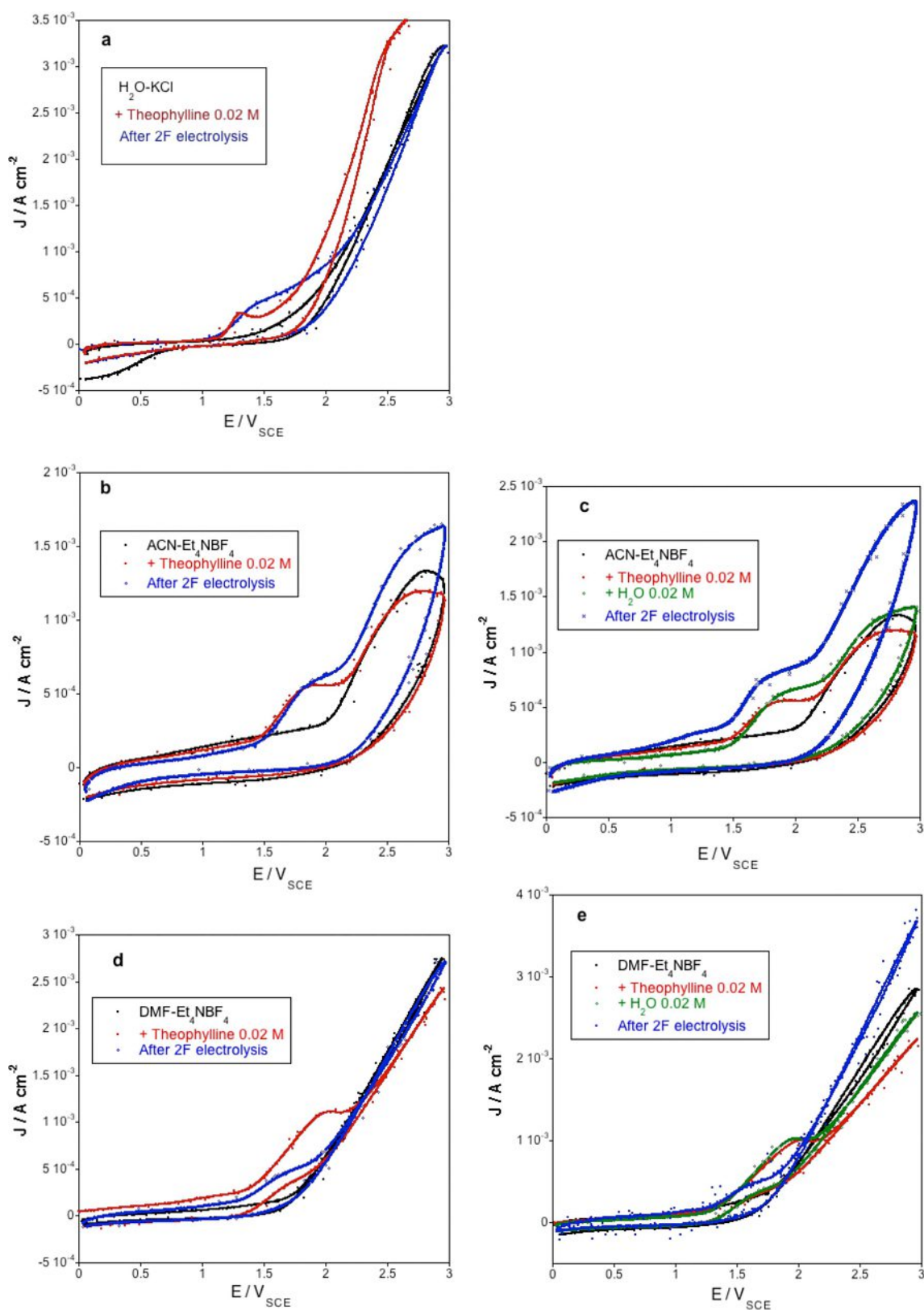


**Figure 2.** Theophylline CVs in various solvent/supporting electrolyte systems. Black: solvent/supporting electrolyte. Red: TPh 0.02 M in solvent/supporting electrolyte. Green: TPh 0.02 M and water 0.04 M in solvent/supporting electrolyte. Blue: after 2F anodic oxidation. GC working electrode, SCE reference electrode, rT,  $\text{N}_2$  atmosphere, scan rate:  $200\text{ mV s}^{-1}$ . a:  $\text{H}_2\text{O}/\text{KCl}$ . b:  $\text{ACN}/\text{Et}_4\text{NBF}_4$ . c:  $\text{ACN}/\text{H}_2\text{O}/\text{Et}_4\text{NBF}_4$ . d:  $\text{DMF}/\text{Et}_4\text{NBF}_4$ . e:  $\text{DMF}/\text{H}_2\text{O}/\text{Et}_4\text{NBF}_4$ .

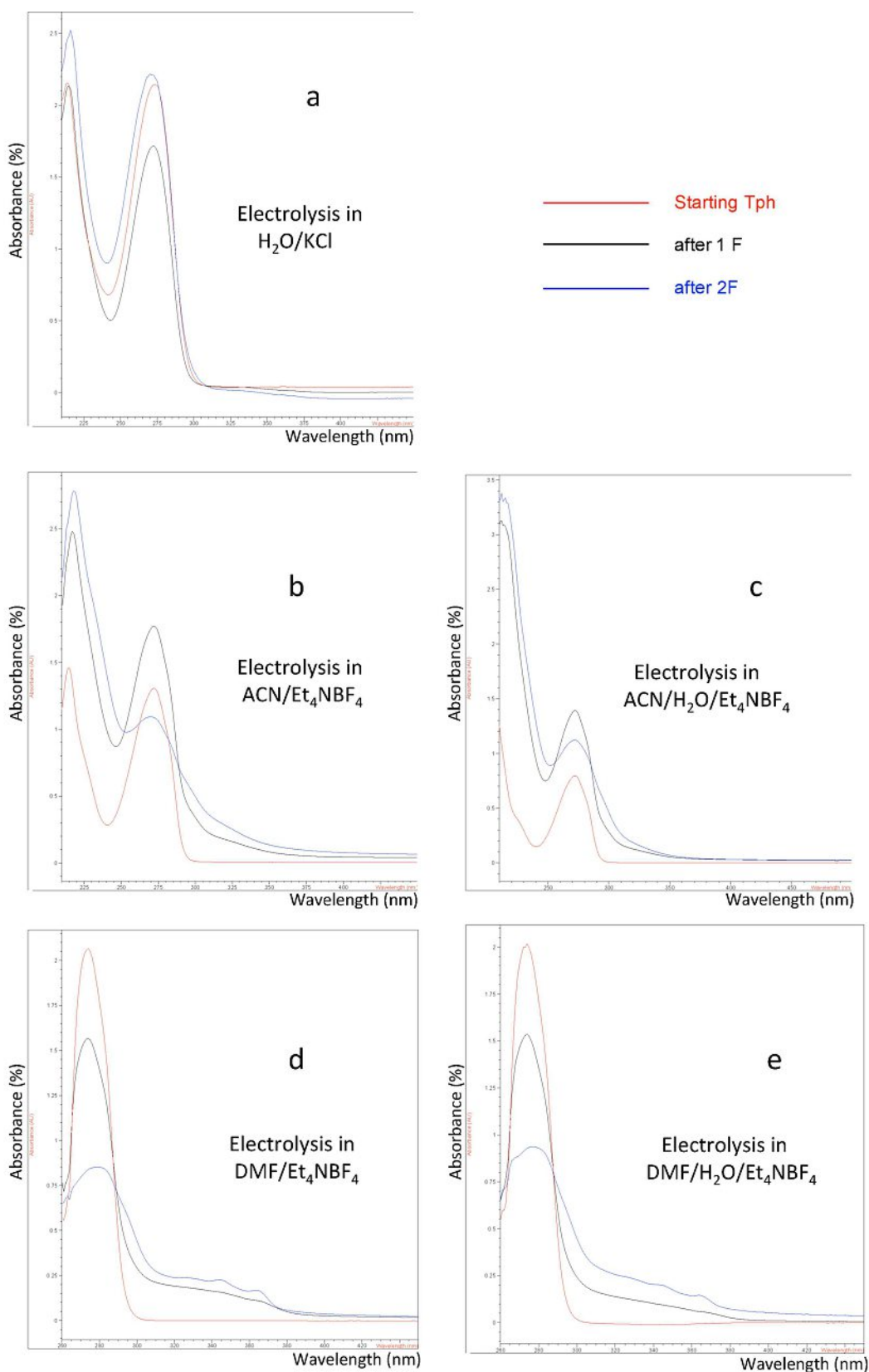


**Figure 3.** TPh UV-Vis spectra in various solvent-supporting electrolyte systems: starting material (red), after 1F (black) and after 2F (blue) anodic oxidation. a:  $\text{H}_2\text{O}/\text{KCl}$ . b:  $\text{ACN}/\text{Et}_4\text{NBF}_4$ . c:  $\text{ACN}/\text{H}_2\text{O}/\text{Et}_4\text{NBF}_4$ . d:  $\text{DMF}/\text{Et}_4\text{NBF}_4$ . e:  $\text{DMF}/\text{H}_2\text{O}/\text{Et}_4\text{NBF}_4$ .

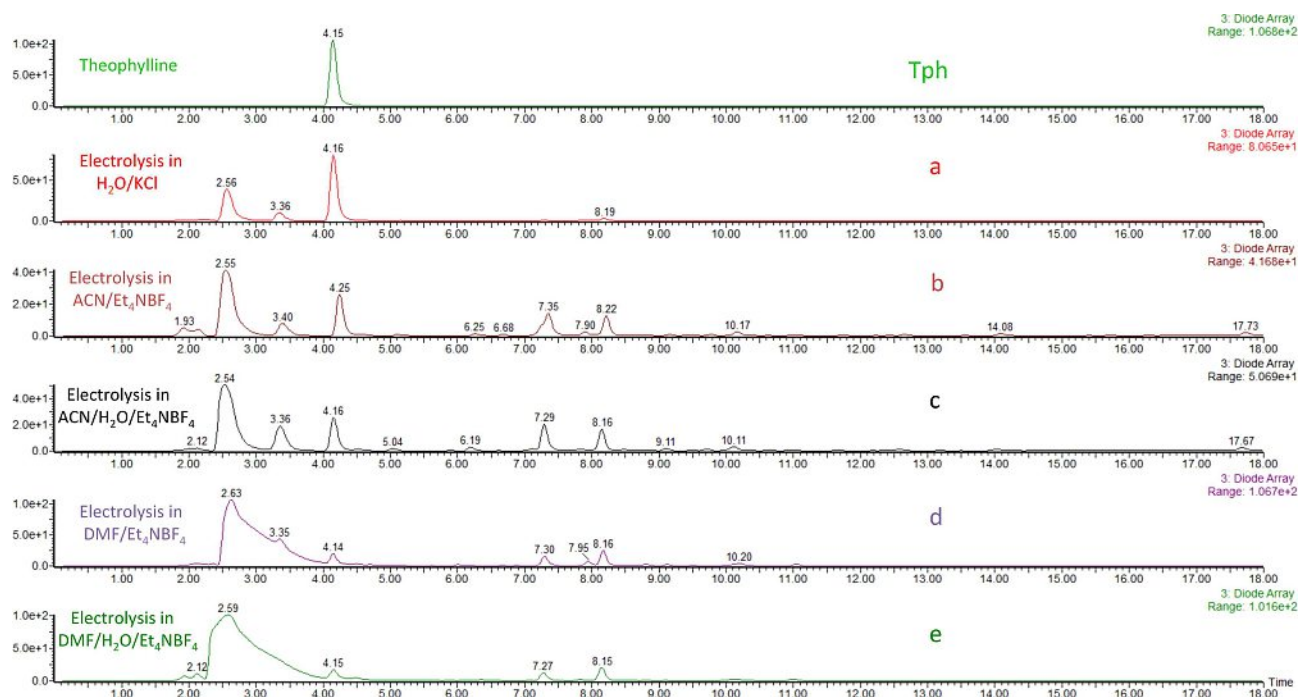


**Figure 4.** PDA chromatograms of starting material (the upper one) and 2F electrolyzed solutions in various solvent-supporting electrolyte systems (a-e). RT = 2.56 min: DMF.

**Table 1.** TPh consumption after 1F and 2F anodic oxidation in various solvent/supporting electrolyte systems.<sup>[a]</sup>

Entry	Medium <sup>[b]</sup>	Faradays <sup>[c]</sup>	Residual TPh <sup>[d]</sup>	Current Efficiency <sup>[e]</sup>
1	H <sub>2</sub> O/KCl	1	94 %	6 %
2	H <sub>2</sub> O/KCl	2	76 %	12 %
3	ACN/Et <sub>4</sub> NBF <sub>4</sub>	1	85 %	15 %
4	ACN/Et <sub>4</sub> NBF <sub>4</sub>	2	27 %	37 %
5	ACN/H <sub>2</sub> O-Et <sub>4</sub> NBF <sub>4</sub>	1	62 %	38 %
6	ACN/H <sub>2</sub> O/Et <sub>4</sub> NBF <sub>4</sub>	2	25 %	38 %
7	DMF/Et <sub>4</sub> NBF <sub>4</sub>	1	73 %	27 %
8	DMF/Et <sub>4</sub> NBF <sub>4</sub>	2	24 %	38 %
9	DMF/H <sub>2</sub> O/Et <sub>4</sub> NBF <sub>4</sub>	1	79 %	21 %
10	DMF/H <sub>2</sub> O/Et <sub>4</sub> NBF <sub>4</sub>	2	22 %	39 %

[a] TPh, RT = 4.15 min,  $[M + H]^+ = 181$ . Electrolysis, chromatographic separation, PDA and ESI-MS/MS detectors conditions: see Experimental. [b] Solvent – 0.1 M supporting electrolyte. TPh concentration: 0.02 M. Water concentration when added to organic solvents: 0.04 M. [c] Faradays per mole of TPh consumed during anodic oxidation. [d] Extracted Ion Chromatogram (EIC) area of residual TPh after 2F vs EIC area of starting material. [e] Current efficiency for a mono-electronic process of TPh.

suggesting a very low current efficiency for the anodic oxidation of TPh in water/KCl on a platinum electrode and a higher current efficiency in organic solvents (as confirmed by chromatographic data). Further, new absorption bands at longer wavelengths, in the range 310–370 nm, were observed after 1F and 2F electrolysis (Figures 3b–e, black line and blue line, respectively) in organic solvents with or without added water, while only a very weak adsorption around 320 nm was observed in water after 2F (Figure 3a, blue line).

These spectrophotometric evidences are consistent with the formation of oxidation products with extended conjugation with respect to the starting TPh, likely TPh dimeric forms, preferentially in organic solvents with respect to water.

In order to have insights on the nature of the products, all the electrolyzed solutions, both after 1F and 2F, were analyzed

by an electrospray ionization tandem mass spectrometry (ESI-MS/MS) detector, in series with a photodiode array (PDA) detector, after chromatographic separation.

Differences between electrolysis in water and in organic solvents could be evidenced by a first view to PDA chromatograms (Figures 4a–e). First, the current efficiency of all electrolysis, both after 1F and after 2F, was calculated on the base of the decreased area of the chromatographic peak at the TPh retention time RT = 4.15 min with respect to the starting TPh (the green upper chromatogram in Figure 4). The values reported in Table 1 confirmed a generally low current efficiency (calculated for a mono-electronic process), ranging around 38% for both organic solvents (Table 1, entries 4, 6, 8, 10, Figures 4b–e), and 12% for water (Table 1, entry 2, Figure 4a).

Second, chromatographic peaks at RTs higher than 4.15 min, that means compounds less polar than TPh, were observed with a very similar profile for electrolysis in organic solvents (with or without added water, Figures 4b–e), while they were absent or at least not detectable for electrolysis in water (Figure 4a). On the contrary, a similar profile for both water and organic solvents was observed at RTs lower than 4.15 min, suggesting the presence of oxidation products with higher polarity (as expected on the base of the polar degradation products of TPh in aqueous medium reported in literature<sup>[10]</sup>).

A multitude of oxidation products for all analyzed samples was better evidenced by Total Ion Chromatograms (TIC) in both negative (nESI) and positive (pESI) full scan mass spectrometry (see Supporting Information, pages 3–4). The main peaks evidenced in both TIC and PDA chromatograms were studied and tentatively assigned.

The main peaks, eluted with TIC RTs of 7.47 min, 8.34 min and 10.26 min, evidenced a  $[M+H]^+$  ion at  $m/z$  393, 378 and 359, respectively, in pESI full scan (see Supporting Information).

Further,  $[M+Na]^+$  and  $[M+K]^+$  adducts at  $m/z$  415 and 431, respectively, were found for  $m/z$  393, and  $[M+Na]^+$  and  $[M+K]^+$  adducts at  $m/z$  400 and 416, respectively, were found for  $m/z$  378. No adducts were found for  $m/z$  359.

All of the three peaks evidenced also a  $[M-H]^-$  ion at  $m/z$  391, 376 and 357, respectively, in nESI full scan (see Supporting Information).

The presence of both  $[M+H]^+$  and  $[M-H]^-$  ions and the adducts, where present, unequivocally indicated compounds with molecular mass 392 Da, 377 Da and 358 Da eluted at RTs 7.47 min, 8.34 min and 10.26 min, respectively, the elution order indicating decreasing polarity.

The presence of isomeric compounds was evidenced by extracting from TIC those molecular masses in both pESI and nESI, a highly selective mode enhancing sensitivity: so, a 392 Da isobaric peak was found at the higher RT=9.27 min (with respect to 7.47 min), not detectable by the less sensitive PDA detector, suggesting a less polar isomeric compound with molecular mass 392 Da. Analogously, a 358 Da isobaric peak was found at the lower RT=8.04 min (with respect to 10.26 min), suggesting a more polar isomeric compound with molecular mass 358 Da. Anyway, the more abundant isomers were definitely those at 7.47 min and 10.26 min, respectively.

The presence of the  $[M-H]^-$  ion for all the assigned masses also suggested the presence of acidic H-atoms in the structures.

The same  $m/z$  values were used as parent mass to get a fragmentation pattern for those compounds by infusion experiments. Different characteristic patterns were found in nESI and pESI (see Supporting Information, pages 7–9), and in all cases fragments evidencing the presence of the starting structural unit of TPh were found (as mass losses of 15 Da and 57 Da). A characteristic fragment  $[M-17]$  was found for compounds with molecular mass 392 Da and 377 Da, suggesting the presence of –OH substituents. The odd molecular mass 377 Da suggested a structure with an odd number of nitrogen atoms.

The UV-Vis spectrum, extracted by the PDA chromatogram, of compounds with masses 392 Da, 377 Da and 358 Da showed a characteristic absorption at  $\lambda_{max}$  286 nm, 286 nm and 310 nm,

respectively, all red shifted with respect to TPh  $\lambda_{max}/274$  nm, likely due to a double bond extended conjugation and/or substitution.

On the base of spectrometric data, elution time order and UV-Vis spectrum, the three main peaks were tentatively assigned to the structures 3–5 reported in Table 2. Mass spectra in pESI and nESI, fragmentation pattern in pESI and nESI and UV-Vis spectrum of each of the suggested dimeric structures 3–5 were shown in Supporting Information (pages 7–9).

A fourth peak eluted with TIC RT of 6.37 min, higher than TPh but lower than the dimers discussed above, evidenced a  $[M+H]^+$  ion with  $m/z$  215, the corresponding  $[M+Na]^+$  and  $[M+K]^+$  adducts at  $m/z$  237 and 253 respectively, and a  $[M-H]^-$  ion with  $m/z$  213 (see Supporting Information, page 6). These data unequivocally indicated a compound with molecular mass 214 Da, and the presence of acidic H-atoms in the structure. The fragmentation pattern by infusion experiments evidenced the mass losses of 15 Da and 57 Da as well as a mass loss of 17 Da, suggesting a TPh structure hydroxyl-substituted. The increase of 34 Da with respect of TPh mass of 180 Da suggested a 2-fold hydroxylation of the starting TPh. The elution time higher than TPh one, in spite of the suggested polar substituents, supported an  $\alpha$ -keto hydroxyl-substitution undergoing an intramolecular H-bond.

The corresponding UV-Vis spectrum showed a characteristic absorption at  $\lambda_{max}/276$  nm, slightly red shifted with respect to TPh, that could be due to a combined effect of lost conjugation and bathochromic substituents. All data, shown in Supporting Information (page 6), suggested the structure 2 reported in Table 2.

The last peak herein discussed was that one eluted with a RT lower than TPh (TIC RT=3.36 min), suggesting a high polarity compound. A  $[M+H]^+$  ion with  $m/z$  223 and a corresponding  $[M-H]^-$  ion with  $m/z$  221 were evidenced (see Supporting Information, page 5), the last one in very low abundance suggesting that the deprotonated form could easily undergo fragmentation in spite of the ESI mild conditions. Three main fragments,  $m/z$  187, 171 and 143 in nESI, were instead well evidenced. The UV-Vis spectrum showed a characteristic absorption at  $\lambda_{max}/233$  nm, consistent with the imidazole unit loss.

Based on these data, the peak at TIC RT of 3.36 min was tentatively assigned to the structure 1, reported in Table 2. All spectrometric data and UV-Vis spectrum were shown in Supporting Information (page 5).

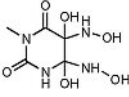
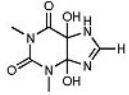
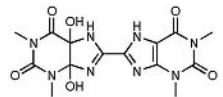
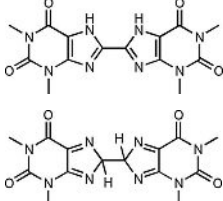
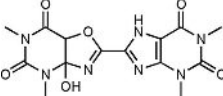
Results relative to the anodic oxidation of TPh in ACN/ $Et_4NBF_4$ , DMF/ $Et_4NBF_4$  and water/KCl, respectively, have been reported separately, as follows.

## 2.1. Theophylline Electro-Oxidation in Acetonitrile

The anodic oxidation of TPh in ACN/ $Et_4NBF_4$ , on a platinum anode at the experimental potential of +2.0 V vs SCE, was noteworthy more efficient than in water (Figure 3b), and TPh conversion was 73 % after 2F (Table 1, entry 4).

The UV-Vis spectra recorded after 1F and 2F evidenced a decrease of the TPh absorption at 272 nm (in ACN) and the

**Table 2.** TPh oxidation main products (tentatively assigned) after 1F and 2F anodic oxidation in various solvent-supporting electrolyte systems on the base of HPLC-PDA-ESI-MS/MS data.<sup>[a]</sup>

Retention Time(s)	M (Da)	Possible Structure(s)	% variation from 1F to 2F <sup>[b]</sup>
3.36	222		H <sub>2</sub> O/KCl: +180% ACN/Et <sub>4</sub> NBF <sub>4</sub> : +102% ACN/H <sub>2</sub> O/Et <sub>4</sub> NBF <sub>4</sub> : +116% DMF/Et <sub>4</sub> NBF <sub>4</sub> : +78% DMF/H <sub>2</sub> O/Et <sub>4</sub> NBF <sub>4</sub> : +90% H <sub>2</sub> O/KCl: +41%
6.37	214		ACN/Et <sub>4</sub> NBF <sub>4</sub> : +70% ACN/H <sub>2</sub> O/Et <sub>4</sub> NBF <sub>4</sub> : +26% DMF/Et <sub>4</sub> NBF <sub>4</sub> : -20% DMF/H <sub>2</sub> O/Et <sub>4</sub> NBF <sub>4</sub> : -47% H <sub>2</sub> O/KCl: +69%
7.47 9.27	392		ACN/Et <sub>4</sub> NBF <sub>4</sub> : +4% ACN/H <sub>2</sub> O/Et <sub>4</sub> NBF <sub>4</sub> : +56% DMF/Et <sub>4</sub> NBF <sub>4</sub> : +109% DMF/H <sub>2</sub> O/Et <sub>4</sub> NBF <sub>4</sub> : +96%
8.04 10.26	358		H <sub>2</sub> O/KCl: -33% ACN/Et <sub>4</sub> NBF <sub>4</sub> : -65% ACN/H <sub>2</sub> O/Et <sub>4</sub> NBF <sub>4</sub> : -54% DMF/Et <sub>4</sub> NBF <sub>4</sub> : -4% DMF/H <sub>2</sub> O/Et <sub>4</sub> NBF <sub>4</sub> : -63%
8.34	377		H <sub>2</sub> O/KCl: -17% ACN/Et <sub>4</sub> NBF <sub>4</sub> : -27% ACN/H <sub>2</sub> O/Et <sub>4</sub> NBF <sub>4</sub> : -2% DMF/Et <sub>4</sub> NBF <sub>4</sub> : +32% DMF/H <sub>2</sub> O/Et <sub>4</sub> NBF <sub>4</sub> : +20%

[a] Electrolysis and chromatography conditions: see Experimental. [b] data obtained from Total Ion Chromatograms in positive ESI mode.

formation of products absorbing in the range 290–350 nm, with two isosbestic points at 260 nm and 285 nm (see Figure 3b).

In accordance, Figure 4b (see also pESI and nESI TICs in Supporting Information) evidenced the presence of the products tentatively assigned to structures 1–5 in Table 2. The % variation for each peak with the progress of electrolysis (from 1F to 2F) was also reported in Table 2. A decrease from 1F to 2F current consumption was found for compound 4, so that the studied oxidation products seemed to derive from dimer 4 (vide infra). Further, because of the presence of hydroxyl-substituted compounds in spite of using anhydrous ACN, water was added to ACN (2 molar excess with respect to TPh) in order to study its effect. Results, shown in Figure 3c and Figure 4c, did not seem so different from those obtained in the same medium without added water (Table 1, entry 4 vs 6). Some differences evidenced by the analysis of % variation data (Table 2) confirmed the role of water in the formation of hydroxylated derivatives.

The degradation product assigned to structure 1 was found with or without added water (Figures 4b and 4c).

## 2.2. Theophylline Electro-Oxidation in *N,N*-Dimethylformamide

The anodic oxidation of TPh was carried out also in DMF/Et<sub>4</sub>NBF<sub>4</sub>, under the same experimental conditions reported for ACN, in the absence and in the presence of added water.

Despite the anodic activity of this dipolar aprotic solvent, probably co-oxidized at the anode (yielding the demethylated product *N*-methylformamide), DMF was chosen due to the higher solubility of TPh in it with respect to other solvents normally used for electro-oxidation.

TPh conversion was found even higher in DMF (78% after 2F, see Table 1, entry 8), and the UV-Vis spectral changes recorded after 1F and after 2F (Figure 3d) evidenced also in this case the formation of products absorbing in the wide range 290–370 nm, with a well detectable isosbestic point at 290 nm.

A similar chromatographic profile was found, as shown in Figure 4 (4d vs 4b), even if the solvent peak hid the first 4 minutes, DMF strongly absorbing around 260 nm. The same elution time range appeared free from solvent interference in pESI and nESI TICs (see Supporting Information, pages 3–4) and well comparable with results in ACN.

Also for electrolysis carried out in DMF, the products tentatively assigned to structures 1–5 in Table 2 were found, and also in this case compound 4 appeared as the first product furtherly reacting to yield the hydroxylated derivatives (see % variation for each peak with the progress of electrolysis reported in Table 2). The presence of water seemed not to affect the general trend, as shown in Table 1, entry 8 vs 10, and in Figures 3e and 4e. Some differences were found by comparing % variation data in DMF vs ACN, as shown in Table 2 (vide infra).



### 2.3. Theophylline Electro-Oxidation in Water

The anodic oxidation of TPh in water/KCl at pH=7, on a platinum working electrode at the experimental anodic potential of +2.0 V vs SCE, occurred with a very low current efficiency, with a large amount of starting material still present after 2F (Table 1, entry 2), as well evidenced by the corresponding UV-Vis spectra (Figure 3d) and PDA chromatogram (Figure 4a).

The highly oxidized small molecule **1** (TIC RT=3.36 min, Table 2) was found as prevalent oxidation product, in accordance with the small molecules reported by Aravindakumar and coworkers<sup>[10]</sup> on the oxidation of TPh induced by hydroxyl radicals, in which no dimeric product was obtained. Moreover, the very low current yield suggested a direct anodic oxidation of water rather than TPh.

Among products **2–5**, only dimer **5** (TIC RT=8.34 min, Table 2) was evidenced by the spectrophotometric detector, as shown in the PDA chromatogram in Figure 4a, but also the other ones were found by extracting the corresponding *m/z* value from TICs in pESI and/or nESI. These data supported the mono-electronic primary anodic oxidation to the radical cation/neutral radical also in aqueous solvent (vide infra). The anodic oxidation of TPh on a pyrolytic graphite electrode in 1 M AcOH, reported by Hansen and Dryhurst,<sup>[13]</sup> yielded the dimer **4** along with the highly oxidized products. The dimer was obtained as a precipitate on the electrode, in 42% chemical yield. The different outcome of our electrochemical oxidation could be due to the different anode material (platinum versus pyrolytic graphite) and/or to the different pH value (2.3 vs 7).

The peak at TIC RT=2.56 min, present also in ACN electrolyzed solutions (Figures 4a-c), was due to DMF because of its presence in the gel dividing the anodic and cathodic compartments.<sup>[22]</sup>

## 3. Discussion

According to the previous study of Petrucci and coworkers<sup>[7]</sup> on the electrochemical behavior of TPh in acetonitrile as aprotic medium, carried out at a GC electrode by cyclic voltammetry,<sup>[7]</sup> the oxidation of TPh occurs through an irreversible mono-electronic primary anodic process yielding the corresponding radical cation, an easy substrate for nucleophiles but also for deprotonation to the neutral radical. So, different competitive chemical reactions may follow the primary anodic oxidation, involving the electrogenerated radical species of TPh. On the other hand, the oxidation of methylxanthines performed in water in general involves up to 4 electrons/mol of substrate, as widely reported in literature.<sup>[13,20]</sup>

In the present work, the anodic oxidation of TPh was carried out in organic solvents to study the reactivity of the electrogenerated TPh radical cation on the base of the obtained oxidation products and results were compared with those obtained in aqueous medium. The electrolyzed mixtures were analyzed by CV, UV-Vis spectrophotometry and mass spectrometry. Although no oxidation product was isolated for a full

characterization due to the multitude of low amount compounds, a quite good chromatographic separation was obtained and some peaks were well characterized by tandem mass spectrometry data.

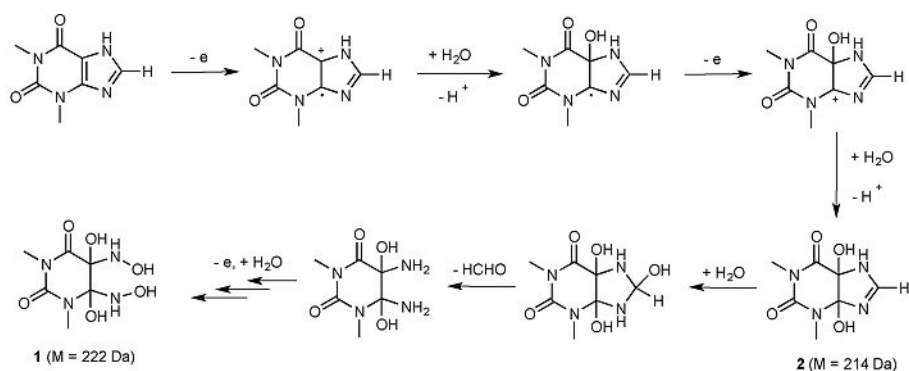
All the experimental data herein reported (and shown in Supporting Information) were consistent with the prevalent formation of dimeric products both in ACN and DMF. Dimeric TPh derivatives were only hardly detected in water. No dimeric TPh derivatives were previously reported, up to our knowledge, excepted compound **4**, isolated in 42% chemical yield as a precipitate on a pyrolytic graphite electrode in water/acetic acid (1 molL<sup>-1</sup>) by Hansen and Dryhurst<sup>[13]</sup>. In that work two structures were proposed for the TPh dimer with *M*=358 Da on the base of IR and UV-Vis spectra, the same structures suggested in the present work and reported in Table 2 as **4a** and **4b**. The red-shift of  $\lambda_{\text{max}}$  from 274 nm of TPh to 310 nm (see Supporting Information, page 8), likely due to the +30 nm double bond extended conjugation,<sup>[23]</sup> strongly supported the structure **4a**. Our experimental data evidenced the formation of dimer **4** in organic solvents. It was detected also in water in trace amount, as reported above, differently from results reported by Hansen and Dryhurst<sup>[13]</sup>: this difference might be likely due to the different pH (2.3 vs 7) and/or to the different anode material (graphite vs platinum).

At the applied anodic potential, dimer **4** could easily be further oxidized: in fact, a decreasing trend along electrolysis was observed for **4** (Table 2, % variation), independently from the used solvent. A corresponding increasing trend was generally observed for the di-hydroxylated dimers with structure **3** or isomers (Table 2, % variation) and dimer **5**, the last being the main dimer found in water (Figure 4a). These data were consistent with UV-Vis spectrum changes (Figures 3b and 3d, black and blue lines) along electrolysis.

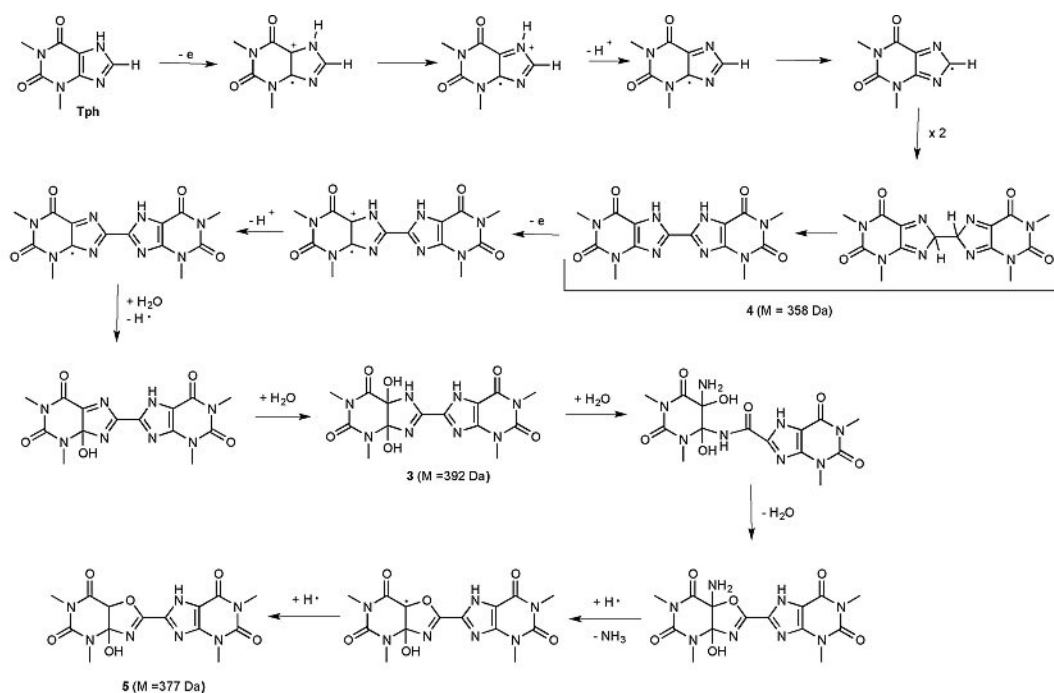
On the other hand, the di-hydroxylated TPh **2** was also found as oxidation product in both ACN and DMF, with or without added water (Figures 4b-e), and trace were also found in water (TIC in Supporting Information), suggesting the formation of an analogous di-hydroxylated derivative by oxidation of dimer **4**.

Oxidation products **2–4** were consistent with the mono-electronic anodic oxidation of the olefinic bond bridging the two rings of TPh molecule, in agreement with what previously proposed and supported by DFT calculation by Petrucci and coworkers,<sup>[7]</sup> leading to a radical cation that can undergo different fate, mainly depending on medium.

In aqueous medium the radical cation might easily undergo nucleophilic attack by water, to form the corresponding hydroxylated radical and the di-hydroxylated TPh **2** after further oxidation at the same anodic potential. Structure **2** had been previously proposed as the product of a possible electrode reaction mechanism,<sup>[15]</sup> but no experimental data to support it have been reported up to our knowledge. The hypothesized mechanism was resumed in Scheme 1. Furthermore, in water hydrolysis of **2** and subsequent oxidation can yield product **1**, as shown in Scheme 1, found as the main oxidation product in water (Figure 4a). On the other hand, the formation of hydroxylamines is a known process when oxidizing amines with



Scheme 1. Hypothesis of mechanism for the formation of oxidation products 1 and 2.



Scheme 2. Hypothesis of mechanism for the formation of oxidation products 3, 4 and 5.

peroxides,<sup>[24,25]</sup> but also the electrochemical oxidation of ammonia in water yields hydroxylamine.<sup>[26]</sup> Compounds 1 and 2, whose structures were based on retention time, mass spectra in both positive and negative ESI full scan, fragmentation pattern and UV-Vis spectrum (see Supporting Information, pages 5 and 6, respectively), formed according to the proposed mechanism (Scheme 1), were also in good accordance with the very low current efficiency (residual Tph after 2F: 76%, Table 1, entry 2) calculated in water on the base of the ratio 1F electrolyzed TPh peak area/starting TPh peak area. In fact, if the low current efficiency in water could be due to the extent in solvation as well as to a scarce selectivity of the electrode process giving the co-oxidation of different electroactive species (most probably water or chloride ion), a low current efficiency was also expected for the multi-electron oxidation process in aqueous medium from the starting TPh to the final degradation product 1.

The radical cation could also undergo deprotonation to the neutral radical, better living in organic solvent,<sup>[27,28]</sup> and coupling reactions might occur. As reported previously,<sup>[7]</sup> C<sup>8</sup> between the two nitrogen atoms of the imidazole ring appeared the most favorite position for the TPh neutral radical, suggesting the formation of dimer 4 (the structure based on retention time, mass spectra in both positive and negative ESI full scan, fragmentation pattern and UV-Vis spectrum, all shown in Supporting Information, page 8), mainly in organic solvents and according to the hypothesized mechanism reported in Scheme 2.

So, the prevalent formation of dimeric compounds in organic solvents vs the prevalent formation of the highly oxidized product 1 in water can be explained on the base of competing reactions involving the TPh neutral radical or the TPh radical cation. ACN and DMF furnish an environment more

favorable to neutral radical species than water, with a prevalent mechanism leading to dimers.

On the other hand, the increasing chromatographic peak of dimer **3** ( $M=392$  Da,  $\Delta=+34$  Da with respect to dimer **4**) along electrolysis evidenced the hydroxylation of **4**, likely occurring with the same mechanistic scheme in Scheme 1 leading first to the radical cation of **4** and followed by a reaction with water (see Scheme 2). The same value of TPH residual amount after 2F found in organic solvents with or without added water suggested the presence of water in spite of the use of anhydrous starting material.

On the base of our results, the chromatographic peak assigned to dimer **5** resulted prevalent or comparable to the peak assigned to dimer **3** after 2F in all the medium tested, water included. The structure of dimer **5** was based on retention time, mass spectra in both positive and negative ESI full scan, fragmentation pattern and UV-Vis spectrum (see Supporting Information, page 9). Further, the odd molecular mass  $M=377$  Da ( $\Delta=-15$  Da with respect to dimer **3**) suggested a structure with the loss of a  $-NH$  unit, according to a reaction pattern for the substitution of the N-atom with the O-atom, after a ring opening and closure, shown in Scheme 2. The presence of **5** in large amount, if compared with the other dimeric structures in water, suggested that also in water the competing coupling reaction can occur, but it undergoes fast further oxidation. In the whole, negligible amounts of dimeric forms were found in water, but their detection well supported the mechanistic considerations in the present work. Moreover, in our experiments 1,3-dimethyluric acid (due to the oxidation of  $C^8$  to carbonyl group) was never formed, despite it was reported as a product when the TPH oxidation was carried out by chemical means.<sup>[12]</sup>

## 4. Conclusions

Theophylline was electrochemically oxidized in organic solvents and in aqueous medium, and the oxidation products were analyzed by an HPLC-PDA-ESI-MS/MS system.

Although no oxidation product was isolated for a full characterization due to the multitude of low amount compounds, a quite good chromatographic separation was obtained and five peaks were well characterized by tandem mass spectrometry and UV-Vis spectrophotometry, strongly supporting compounds **1–5** as the main products of the electrochemical oxidation of TPH.

A prevalent formation of dimeric products was found in organic solvents: two of the three suggested structure **3–5**, namely **3** and **5**, had not been previously reported.

A prevalent formation of the suggested highly oxidized product **1**, not previously reported, was found in water. The suggested di-hydroxylated TPH derivative **2** had been previously proposed but no experimental evidence has been given up to our knowledge. All compounds **1–5** were found both in organic and aqueous medium, supporting the mono-electronic anodic oxidation of the olefinic bond of TPH to the corresponding radical cation regardless of the environment, followed by

different competing chemical reactions depending on the solvent. In particular, TPH degradation products seemed to prevail in aqueous medium, in good agreement with literature on the chemical oxidation of TPH in water, while dimers seemed to prevail in organic solvent, a more lipophilic environment that could easily mimic body fluids and biological membranes.

Hypothesis of mechanism for the formation of all the oxidation products, whose structures were suggested and supported by our experimental data, were given.

The mild conditions of the electrochemical oxidation of TPH as well as the “controlled electron number” electrolysis in organic solvents allowed to study the reactivity of the electro-generated theophylline radical cation and put in evidence intermediates which were never evidenced after chemical oxidation (usually carried out under harsh conditions), directing the reaction towards the formation of dimeric species instead of directly to highly oxidized monomeric ones, thus shedding some lights on the reaction mechanism.

## Experimental Section

### Materials

All reagents were commercially available and used as received (anhydrous ACN and DMF were used).  $Et_4NBF_4$  was used after being kept at reduced pressure at 70 °C for 24 h. Formic acid (98%) was purchased from Sigma-Aldrich; HPLC grade acetonitrile was purchased from Carlo Erba (Milano, Italy); HPLC grade water was prepared with the Milli-Q purification system (Millipore, Vimodrone, Italy).

### Voltammetric Measurements

Voltammetric measurements were performed using an Amel 552 potentiostat equipped with an Amel 566 function generator and an Amel 563 multipurpose unit in a three-electrode cell; the curves were displayed on an Amel 863 recorder; acquisition software was a CorrWare for windows version 2.8d1 Scribner, elaboration software was a CorrView for windows version 2.8d1 Scribner. A 492/GC/3 Amel microelectrode was employed, using a Pt wire counter electrode and a modified saturated calomel electrode as reference electrode (mSCE: SCE with organic solvent junction; the oxidation peak potential of ferrocene measured on GC electrode in DMF containing 0.1 M  $Et_4NBF_4$  as supporting electrolyte, is  $E_{oxFc} = +0.512$  V vs mSCE). A normal SCE was used when the solvent was water. The scan rate was  $\nu = 0.200$  V  $s^{-1}$ . All cyclic voltammeteries were recorded at room temperature on 5 mL of solvent/0.1 M supporting electrolyte.

### Controlled Potential Electrolyses

Constant potential electrolyses ( $E = +2.0$  V, vs SCE) were performed under a nitrogen atmosphere, at room temperature, using an Amel Model 552 potentiostat equipped with an Amel Model 731 integrator. All the experiments were carried out in a divided glass cell separated through a porous glass plug filled up with a layer of gel (i.e., methyl cellulose 0.5% vol dissolved in DMF/ $Et_4NBF_4$  0.1 M or  $H_2O/DMF/KCl$  0.1 M in case of electrolysis in water); Pt spirals (apparent area 0.8  $cm^2$ ) were used as both cathode and anode. Anolyte: 5 mL of solvent containing 0.10 mmol of TPH. Catholyte: 2 mL of the same solvent of anolyte. After 10 C (corresponding to

1F), a portion of the anolyte was sampled and analyzed. After 20 C (corresponding to 2F) the current flow was stopped, and the anolyte was analyzed.

### UV-Vis Experiments

UV-Vis experiments were carried out with an Agilent 8453 diode array spectrophotometer. Samples for UV-Vis spectrum recording were prepared as follows: aliquots of 30  $\mu\text{L}$  were withdrawn from the starting solution, 1F electrolyzed solution and 2F electrolyzed solution, respectively, and then diluted 1:100 with the corresponding solvent (ACN, DMF or water).

### HPLC-PDA-ESI-MS/MS Analysis

Chromatographic separation was performed by an HPLC separation module 1525  $\mu\text{ Waters (Milford, MA, USA) using a Waters XBridge C18 (150}\times\text{2.1 mm i.d.) 5 }\mu\text{m analytical column, A (water/formic acid 0.02\%)} and B (acetonitrile/formic acid 0.02\%) as mobile phase, and a flow rate of 0.20 mL min}^{-1}. The elution gradient was as follows: 0–20 min, 5–60\% B; 20–30 min, 60\% B; 30–32 min, 60–5\% B; 32–52 min, 5\% B.$

A Waters 996 photodiode array (PDA) detector was set for one spectrum per second in the range 200–600 nm.

The separation system was linked to a Quattro Micro Tandem MS-MS with an electrospray ionization (ESI) source Waters (Micromass, Manchester UK). Data were acquired in full scan both in positive (pESI) and negative (nESI) modes, in the mass range 135–500 Da, with the following ESI source parameters: capillary voltage 3000 V, cone voltage 25 V, source temperature 120  $^{\circ}\text{C}$ , desolvation temperature 350  $^{\circ}\text{C}$ , cone gas flow 40  $\text{L h}^{-1}$ , desolvation gas flow 600  $\text{L h}^{-1}$ . Data acquisition, data handling and instruments control were performed by MassLynx Software 4.1 v (Data Handling System for Windows, Micromass, UK).

Samples were prepared by diluting (1:100) 10  $\mu\text{L}$  of the electrolyzed solutions, in turn, with mobile phase A:B (95:5, v:v) and the filtrate (Cronus Syringe Filter 0.45  $\mu\text{m}$ ) injected (20  $\mu\text{L}$ ) for the analysis. All the samples were analyzed in duplicate in two independent runs.

The Total Ion Chromatograms (TIC) in pESI were extracted at the  $[\text{M} + \text{H}]^{+}$  of TPh,  $m/z = 181$ , and the corresponding peak areas were measured for current efficiency calculation.

Infusion experiments were carried out in daughter mode, both in pESI and nESI, using argon as collision gas. The same samples, prepared as described above, were infused directly into the source using an external syringe pump with a set flow rate of 5  $\mu\text{L min}^{-1}$ , selecting the parent ion in turn and optimizing the collision energy (CE) value to obtain the corresponding best fragmentation pattern. In detail:  $[\text{M} + \text{H}]^{+} = 215$  CE 23 eV and  $[\text{M} - \text{H}]^{-} = 213$  CE 25 eV;  $[\text{M} + \text{H}]^{+} = 359$  CE 28 eV and  $[\text{M} - \text{H}]^{-} = 357$  CE 28 eV;  $[\text{M} + \text{H}]^{+} = 378$  CE 15 eV and  $[\text{M} - \text{H}]^{-} = 376$  CE 15 eV;  $[\text{M} + \text{H}]^{+} = 393$  CE 15 eV and  $[\text{M} - \text{H}]^{-} = 391$  CE 17 eV.

### Acknowledgements

This work was financially supported by Sapienza University of Rome. The authors want to thank Mr. Marco Di Pilato for technical support.

### Conflict of Interest

The authors declare no conflict of interest.

**Keywords:** theophylline · anodic oxidation · cyclic voltammetry · mass spectrometry · UV-Vis spectrophotometry

- [1] J. Monteiro, Marco G. Alves, Pedro F. Oliveira, Branca M. Silva, *Crit. Rev. Food Sci. Nutr.* **2019**, in press. <https://doi.org/10.1080/10408398.2018.1461607>.
- [2] J.-F. Chen, Y. Chern in *Methylxanthines*, Springer, Berlin Heidelberg, **2011**, pp. 267–310.
- [3] J. Monteiro, M. Alves, P. Oliveira, B. Silva, *Molecules* **2016**, *21*, 974, doi:10.3390/molecules21080974.
- [4] P. J. Barnes, *Am. J. Resp. Crit. Care Med.* **2013**, *188*, 901–906.
- [5] S. Azam, N. Hadi, N. U. Khan, S. M. Hadi, *Med. Sci. Monit.* **2003**, *9*, 325–330.
- [6] J. R. Leon-Carmona, A. Galano, *Int. J. Quantum Chem.* **2012**, *112*, 3472–3478.
- [7] R. Petrucci, G. Zollo, A. Curulli, G. Marrosu, *BBA-General Subjects* **2018**, *1862*, 1781–1789.
- [8] S. Nanjundiah, P. Bhatt, N. K. Rastogi, M. S. Thakur, *Appl. Biochem. Biotechnol.* **2016**, *178*, 58–75.
- [9] Y. Vystavna, F. Huneau, V. Grynenko, Y. Vergeles, H. Celle-Jeanton, N. Tapie, H. Budzinski, P. Le Coustumer, *Water Air Soil Pollut.* **2012**, *223*, 2111–2124.
- [10] M. M. S. Paul, U. K. Aravind, G. Pramod, A. Saha, C. T. Aravindakumar, *Org. Biomol. Chem.* **2014**, *12*, 5611–5620.
- [11] Z. T. How, K. L. Linge, F. Buseti, C. A. Joll, *Environ. Sci. Technol.* **2017**, *51*, 4870–4876.
- [12] S. Sun, J. Jiang, S. Pang, J. Ma, M. Xue, J. Li, Y. Liu, Y. Yuan, *Sep. Pur. Technol.* **2018**, *201*, 283–290.
- [13] B. H. Hansen, G. Dryhurst, *Electroanal. Chem. Interfac. Electrochem.* **1971**, *32*, 405–414.
- [14] A. A. Reskety, M. A. Chamjangali, M. Boujnane, A. Brajter-Toth, *Electroanalysis* **2016**, *28*, 2506–2513.
- [15] S. D. Bukkitgar, N. P. Shetti, *Mat. Today: Proceed.* **2018**, *5*, 21474–21481.
- [16] F. Pandolfi, L. Mattiello, D. Zane, M. Feroci, *Electrochim. Acta* **2018**, *280*, 71–76.
- [17] F. Pandolfi, I. Chiarotto, L. Mattiello, D. Rocco, M. Feroci, *Synlett* **2019**, *30*, 1215–1218.
- [18] K. K. Chan, R. Ganguly, Y. Li, R. D. Webster, *ChemElectroChem* **2014**, *1*, 1557–1562.
- [19] I. Iftikhar, A. Brajter-Toth, *Electroanalysis* **2015**, *27*, 2872–2881.
- [20] B. H. Hansen, G. Dryhurst, *Electroanal. Chem. Interfac. Electrochem.* **1971**, *30*, 417–426.
- [21] A. Trani, R. Petrucci, G. Marrosu, D. Zane, A. Curulli, *J. Electroanal. Chem.* **2017**, *788*, 99–106.
- [22] G. Sotgiu, I. Chiarotto, M. Feroci, M. Orsini, L. Rossi, A. Inesi, *Electrochim. Acta* **2008**, *53*, 7852–7858.
- [23] R. M. Silverstein, G. C. Bassler, T. C. Morrill, *Spectrometric identification of organic compounds*, John Wiley&Sons, Inc., New York, 5<sup>th</sup> Ed., **1991**, p. 298
- [24] J. D. Fields, P. J. Kropp, *J. Org. Chem.* **2000**, *65*, 5937–5941
- [25] A. Banerjee, H. Yamamoto, *Chem. Sci.* **2019**, *10*, 2124–2129
- [26] N. J. Bunce, D. Bejan, *Electrochim. Acta* **2011**, *56*, 8085–8093
- [27] R. Petrucci, P. Astolfi, L. Greci, O. Firuzi, L. Saso, G. Marrosu, *Electrochim. Acta* **2007**, *52*, 2461–2470
- [28] R. Petrucci, L. Saso, V. Kumar, A. K. Prasad, S. V. Malhotra, V. S. Parmar, G. Marrosu, *Biochimie* **2010**, *92*, 1123–1129

Manuscript received: June 26, 2019  
Revised manuscript received: July 26, 2019  
Accepted manuscript online: August 7, 2019